Neurobiology of Aging 137 (2024) 47–54

Contents lists available at ScienceDirect

Neurobiology of Aging

journal homepage: www.elsevier.com/locate/neuaging.org

Data-driven analysis of regional brain metabolism in behavioral frontotemporal dementia and late-onset primary psychiatric diseases with frontal lobe syndrome: A PET/MRI study

Annachiara Cagnin [a,b,*], Giorgio Pigato [c], Ilaria Pettenuzzo [a], Giovanni Zorzi [a,b,d], Beatrice Roiter [c], Maria Giulia Anglani [e], Cinzia Bussè [a], Stefano Mozzetta [a], Carlo Gabelli [d], Cristina Campi [f,g], Diego Cecchin [b,f]

[a] Neurology Unit, Department of Neuroscience (DNS) University of Padua, Padua, Italy
[b] Padua Neuroscience Center, University of Padua, Padua, Italy
[c] Psychiatry Unit, Department of Neuroscience (DNS), University of Padua, Padua, Italy
[d] CRIC, Azienda Ospedale-Università of Padua, Italy
[e] Neuroradiology Unit, University of Padua, Padua, Italy
[f] Nuclear Medicine Unit, Department of Medicine (DIMED), University of Padua, Padua, Italy
[g] Department of Mathematics, University of Genoa and IRCCS Policlinico San Martino Hospital, Genoa

ARTICLE INFO

Keywords:
Frontotemporal lobar degeneration
Frontotemporal dementia
PET
Metabolism
Phenocopy
Psychiatric diseases

ABSTRACT

Late-onset primary psychiatric disease (PPD) and behavioral frontotemporal dementia (bvFTD) present with a similar frontal lobe syndrome. We compare brain glucose metabolism in bvFTD and late-onset PPD and investigate the metabolic correlates of cognitive and behavioral disturbances through FDG-PET/MRI. We studied 37 bvFTD and 20 late-onset PPD with a mean clinical follow-up of three years. At baseline evaluation, metabolism of the dorsolateral, ventrolateral, orbitofrontal regions and caudate could classify the patients with a diagnostic accuracy of 91% (95% CI: 0.81–0.98%). 45% of PPD showed low-grade hypometabolism in the anterior cingulate and/or parietal regions. Frontal lobe metabolism was normal in 32% of genetic bvFTD and bvFTD with motor neuron signs. Hypometabolism of the frontal and caudate regions could help in distinguishing bvFTD from PPD, except in cases with motor neuron signs and/or genetic bvFTD for which brain metabolism may be less informative.

1. Introduction

Behavioral variant frontotemporal dementia (bvFTD) is the most common clinical phenotype of frontotemporal lobe degeneration. Characteristics that define a diagnosis of possible bvFTD are behavioral changes such as disinhibition and/or apathy, repetitive behavior, hyperorality, social cognition deficits with lack of insight, and executive deficits over time (Rascovsky et al., 2011). Neuroimaging detection of frontotemporal atrophy and/or hypometabolism can increase accuracy in identifying neurodegenerative cases, and allows the diagnosis of bvFTD to be upgraded from possible to probable if functional decline over time is detected.

Diagnosing bvFTD is challenging as its core clinical features are common to many heterogenous disorders ranging from neurological diseases with focal lesions of the frontal lobe to late-onset primary psychiatric diseases (PPD). Many different psychiatric disorders, i.e. affective or personality disorders, could present with frontal lobe behavioral changes, and therefore may be considered possible bvFTD (Vijverberg et al., 2017).

Recommendations to help distinguish between bvFTD and PPD were recently published (Ducharme et al., 2020). Conditions in favor of a diagnosis of bvFTD are (a) presence of familial neuropsychiatric disturbances, (b) exclusion of a DSM-5 diagnosis of primary psychiatric disorder, and (c) presence of motor neuron or extrapyramidal signs at neurological examination. The expert panel proposed supplementing the diagnostic work-up with tests of social cognition, dedicated behavioral scales, assessment of MR brain images using standardized visual rating scales or volumetric analyses. Nuclear medicine neuroimaging is

* Corresponding author at: Neurology Unit, Department of Neuroscience (DNS), University of Padua, Padua, Italy.
E-mail address: annachiara.cagnin@unipd.it (A. Cagnin).

https://doi.org/10.1016/j.neurobiolaging.2024.01.015
Received 10 July 2023; Received in revised form 10 January 2024; Accepted 30 January 2024
Available online 3 February 2024

recommended when structural imaging is not resolutive and diagnostic uncertainty persists.

It has been observed that certain neuroimaging features required for a diagnosis of bvFTD may be absent in some genetic forms of bvFTD (Devenney et al., 2014; Mahoney et al., 2012; Whitwell et al., 2012), yet may be present in patients with non-neurodegenerative late-onset frontal lobe syndrome (Vijverberg et al., 2017). Application of neuroimaging to validate a bvFTD diagnosis could therefore result in some patients with genetic bvFTD being given a false-negative diagnosis, and some with late-onset frontal lobe syndrome, such as some cases of PPD, being given a false-positive diagnosis. The strongest predictor of bvFTD versus its mimickers is the absence of cognitive and functional decline over at least one year of observation. However, this leaves a period of diagnostic uncertainty in possible bvFTD cases with atypical neuroimaging findings at first assessment.

We studied a group of patients with late-onset frontal lobe syndrome due to bvFTD or PPD in order to (1) detect the heterogeneity of spatial patterns of glucose hypometabolism, (2) assess the specific features of PPD mimicking bvFTD and atypical features of bvFTD, and (3) detect the metabolic correlates of cognitive and neuropsychiatric symptoms.

2. Methods

2.1. Study population

Patients were recruited at the outpatient memory clinic of the Department of Neuroscience in Padua (Italy) between 2011 and 2020. Fifty-seven subjects with late-onset behavioral impairment with predominant frontal lobe syndrome and satisfying the current criteria of possible bvFTD (Rascovsky et al., 2011) were selected for the study. Inclusion criteria were: baseline MMSE score $>$ 15/30, and language and behavioral difficulties not interfering with the neuropsychological assessment. Exclusion criteria were: a previous diagnosis of a primary psychiatric disorder or other neurological disease causing behavioral and/or cognitive impairment, and contraindication to undergo a FDG-PET/MRI scan. Past medical history and previous consultations with a psychiatric service or neurological unit were verified with a review of the patients' medical charts or through the national health system database.

After an extensive diagnostic work-up and follow-up visits, patients were diagnosed with either bvFTD (n = 37) or PPD (n = 20). Probable bvFTD was diagnosed in 31 patients, and definite bvFTD in 6 patients after documenting a pathogenetic gene mutation (4 c9orf72 expansion and 2 GRN gene mutation) and according to diagnostic criteria for bvFTD (Rascovsky et al., 2011).

PPD was diagnosed according to DSM-5 criteria with the following conditions also met: normal brain MRI scan and lack of functional impairment (not worsening after at least one year of follow up).(Kipps et al., 2010) The following psychiatric diagnoses were made: late-onset bipolar disorder (BD) (n = 9: 7 type II, and 2 type I), unipolar depressive disorder (UDD) (n = 3), personality disorder (PD) (n = 3, type B), generalized anxiety disorder (GAD) (n = 4), schizophrenic disorder (SD) (n = 1).

2.2. Clinical assessment

All patients underwent a multidisciplinary assessment at baseline with a neurologist (formal neurological examination, UPDRS (Goetz et al., 2007) scale for extrapyramidal symptoms) and a psychiatrist (Mini-International Neuropsychiatric Interview) (Sheehan et al., 1998), brain MRI, FDG-PET/MRI brain scan, and genetic testing for pathogenetic mutations of bvFTD (c9orf72, GRN, TAU). All patients attended follow-up visits for a minimum of 12 months, with a mean follow-up time of 35.23 ± 14.21 months (range 12–61 months). Clinicians were blind to the results of FDG-PET which was made available after the 1-year follow-up visit.

All participants were assessed for behavioral disorders with the Neuropsychiatric Inventory (NPI) (Cummings et al., 1994) and the Stereotypic and Ritualistic Behavior-revised (SRB-r) (Cagnin et al., 2014) questionnaires to quantify the frequency and severity of verbal and motor stereotypies and recurrent ritual behaviors.

Neuropsychological evaluation was carried out with the MMSE, digit cancellation test (Della Sala et al., 1992), Trail Making Test A (TMT-A) for visual attention, digit span forward and backward for short-term and working memory, the prose memory test and Rey Auditory Verbal Learning Test (RAVLT) (Carlesimo et al., 1996) for episodic memory, verbal fluency for lexical access and executive functions, the Frontal Assessment Battery (FAB) (Dubois et al., 2000) for executive memory, clock drawing test for visual-constructional abilities, and the Rey-Osterrieth Complex Figure (ROCF) test for visual-constructional abilities (copy) and long-term visuo-spatial memory (delayed recall) (Caffarra et al., 2002). Functional abilities were evaluated with the Activities of Daily Living (ADL) (Katz et al., 1963) and the Instrumental Activities of Daily Living (iADL) (Lawton and Brody, 1969) scales.

The local ethics committee approved the study, and written informed consent was obtained from all participants (protocol number 0038879).

2.3. Imaging study

In accordance with the EANM guidelines for neurodegenerative diseases (Varrone et al., 2009), after fasting for about 8 h subjects were given an intravenous injection of 3 MBq/kg of 18 F-FDG (using a Medrad Intego PET infusion system) in a quiet, dimly lit room. No significant hyperglycemia was detected ($<$150 mg/dl) before injection. Patients were instructed not to speak, read or be otherwise active during the uptake period (about 25 min) and to keep their eyes closed.

One hour after injection, images were acquired (PET scan duration 25 min) using a 3 T PET/MRI system (Biograph mMRl, Siemens, Erlangen, Germany). A radial VIBE (UTE) sequence (1.6×1.6×1.6 mm) was used to generate attenuation coefficient maps.

PET images were reconstructed to a 344×344 matrix (voxel size 2.08×2.08×2.03 mm) using a single (25 min) frame and the built-in 3D ordered subset expectation maximization algorithm with 8 iterations and 21 subsets. Standard corrections for decay, scatter, and dead time were performed. A number of anatomical data (MRI) were also obtained simultaneously with PET acquisition (3D T1, 3D Flair, DWI, SWI, Axial T2 TSE).

2.4. MRI assessment

Brain atrophy and cerebrovascular abnormalities were visually assessed jointly by an experienced neuroradiologist and a nuclear medicine physician.

Cerebral atrophy was evaluated on the axial T2-weighted sequence and graded using the global cortical atrophy (GCA) scale, also known as the Pasquier scale, which assesses atrophy in 13 regions: dilation of the right and left frontal, parieto-occipital and temporal sulci, dilation of the right and left frontal, parieto-occipital and temporal ventricles and dilation of the third ventricle. The scores range from 0 (no atrophy/dilation) to 3 ("knife blade" atrophy with severe ventricular enlargement) (Pasquier et al., 1996).

Medial temporal lobe atrophy (MTA) was evaluated on the coronal T1-weighted plane images and graded using a standardized scale on the basis of the width of the choroid fissure, enlargement of the temporal horn of the lateral ventricle, and the height of the hippocampus. The right and left sides were rated separately. Scores range from 0 (no atrophy) to 4 (severe atrophy) (Scheltens et al., 1995, 1992).

Posterior cortical atrophy (PCA) was graded using the Koedam scale on the basis of the width of the posterior cingulate and parieto-occipital sulci, and the height of the precuneus gyrus and parietal cortex in three orientations (sagittal, coronal and axial). The right and left sides were rated separately. Koedam scores range from 0 (no atrophy) to 3 (marked

sulcal widening and severe gyrus atrophy) (Koedam et al., 2011).

The Fazekas scale was used to evaluate white matter hyperintense signal abnormalities surrounding the ventricles and in the deep white matter associated with small vessel ischemia. Hyperintensity was graded according to the size and confluence of the lesions from 0 (absent) to 3 (confluent areas/extending into the deep white matter) (Fazekas et al., 1987).

2.5. 18 F-FDG-PET assessment

A nuclear medicine physician (with more than 10 years' experience reading images in cases of neurodegenerative disease) qualitatively evaluated the PET/MR images using the Siemens SyngoVia software. An age-matched database was also used for semi-quantitative evaluation of metabolism using 3D-SSP analysis.(Minoshima et al., 1995) We used the "FDG2A database FDG-PET Biograph (age range 46–79)" implemented in Syngo.via with cerebellum + Vermis (AAL) as normalization region.

For the aims of the present paper, part of a method previously proposed (Cecchin et al., 2017) was then used to correct the PET images for partial volume effect (PVE) using the T1-MPRAGE sequence of the same patient. We obtained 111 cortical and subcortical volumes of interest (VOI) corrected for PVE. Levels of SUVr (Standardized Uptake Value ratio) were then obtained for each VOI using pons as the reference region.

2.6. Statistical analysis

Differences in the demographic and clinical data and the radiological indices were assessed with an ANOVA for continuous variables and the Mann-Whitney U test as appropriate. Fisher's Exact Test was used for categorical variables. MMSE was considered a nuisance covariate factor. A significance level of $\alpha = 0.05$ was adopted. Results were considered statistically significant when $p \leq 0.05$, and false discovery rate (FDR) multiple comparison correction was performed where appropriate. Principal Component Analysis (PCA) (Hotelling, 1933) was performed on the dataset to investigate the distribution of the population and the contribution of the different SUVr areas. The regions that contributed to the first principal component explaining the largest part of the variance were used to build a linear regression model to classify bvFTD from PPD patients. The performance of the model was assessed using score metrics and Receiver Operating Curve (ROC).

The analyses were performed using R 3.6.

3. Results

3.1. Clinical and instrumental findings

The demographic and clinical characteristics of the two groups are presented in Table 1.

The bvFTD and PPD groups were comparable for age ($p = 0.98$), sex distribution ($p = 0.31$), age at disease onset ($p = 0.71$), educational level ($p = 0.71$), disease duration ($p = 0.16$), and follow-up period ($p = 0.44$). Patients with bvFTD had a lower mean MMSE score (bvFTD: 23.68 ± 3.40; PPD: 25.89 ± 3.05; $p = 0.02$). Signs of motor neuron involvement were present at baseline in 7/37 (19%) of bvFTD patients, and in none of the PPD patients.

Cognitive tests scores are reported in Table 1 of Supplemental Materials: bvFTD patients performed similarly to PPD in all cognitive tests. There was a trend of bvFTD performing worse on immediate prose memory ($p = 0.04$), delayed visual memory ($p = 0.02$), and working memory ($p = 0.04$), but it did not survive multiple comparison correction.

The overall burden of behavioral disorders was similar in the bvFTD and PPD groups (mean NPI-total scores: bvFTD, 34.47 ± 18.37; PPD, 26.20 ± 14.31; $p = 0.7$), but the severity of compulsive symptoms was greater in the bvFTD group (mean SRB-r scores: bvFTD, 18.34 ± 13.40; PPD, 10.00 ± 10.22; $p = 0.01$), particularly in the subitems "counting" and "leisure activities" (Supplemental Materials Table 2). Mean NPI scores for the apathy, disinhibition, and eating changes items were higher in bvFTD, but for the depression and anxiety items they were higher in PPD.

Table 1
Demographic and clinical characteristics.

Variables	bvFTD n = 37	PPD n = 20	P (T/U-test/χ2)
Sex, male n (%)	18 (48.65)	7 (35)	0.31
Age, mean ± SD	66.51 ± 8.71	66.45 ± 9.56	0.98
Age at onset, mean ± SD	60.81 ± 9.76	61.85 ± 10.22	0.71
Disease duration (yrs), mean ± SD	2.73 ± 1.24	2.25 ± 1.21	0.16
Follow up (months), mean ± SD	36.03 ± 15.05	31.80 ± 15.89	0.44
Family history, yes, n (%)	17 (45.9)	9 (45)	0.94
Previous psychiatric events	18 (48.65)	15 (75)	0.054
MMSE score, mean ± SD	23.68 ± 3.40	25.89 ± 3.05	**0.02**
NPI total score	34.47 ± 18.37	26.20 ± 14.31	0.07
SRB-r total score	18.34 ± 13.40	10.00 ± 10.22	**0.01**
MRI characteristics, median (IQR)			
Global cortical atrophy	2 (1.5)	1 (0.13)	**< 0.001** *
Medial temporal atrophy R/L	1/2 (1.5/2)	0/0 (0/0.13)	**< 0.001** *
Posterior cortical atrophy R/L	1/1 (1/0.5)	0/ 0 (1/0.63)	0.19/**< 0.01** *
WMH, Fazekas	0 (1)	0 (1)	0.81
FDG-PET pattern, median (IQR)			
Frontal lobe (R/L)	1/2 (3/2)	0/0 (0.25)	**< 0.01** * /< **0.001** *
Temporal lobe (R/L)	0/2 (1/3)	0/0 (0)	0.21/**< 0.001** *
Parietal (R/L)	0/1(1/2)	0/0 (0.25)	0.86/**0.04**
Normal n (%)	4 (11)	11(55)	<0.001

Abbreviations: MMSE: Mini-Mental State Examination; NPI, Neuropsychiatry Inventory questionnaire; SRB-r, Stereotypic and Ritualistic Behavior–revised questionnaire; WMH, White Matter Hyperintensity. *Significant after FDR

Visual ratings of the brain MRIs revealed differences between bvFTD and PPD, with greater overall and focal temporal atrophy in bvFTD patients, mainly on the left side, although they had almost comparable signs of parietal atrophy and absent white matter abnormalities (Table 1).

Qualitative analysis of the FDG-PET images showed that 4/37 bvFTD patients had an almost normal scan, while the majority of abnormal scans showed frontal hypometabolism (30/33, 90%) and temporal hypometabolism (25/33, 76%). In 3 cases the abnormality was isolated in the temporal regions. Patients with genetic bvFTD had heterogeneous patterns of hypometabolism: c9orf+ had frontal hypometabolism (n = 3) with parietal extension in one case, and one had an almost normal scan; GRN mutations had frontal hypometabolism (n = 2/2) with extension to the parietal cortex in one case.

Nine out of 20 (45%) PPD patients showed some degree of regional cortical hypometabolism at visual inspection: the anterior cingulate was involved in 5 cases, and parietal regions in 5 cases, 3 of which were with extension to the temporal regions. PPD patients with abnormal cortical metabolism were older respect to those with normal brain scan (mean age: 69.7 ± 5.8 versus 59.6 ± 8.7 years, $p = 0.005$). No other differences were detected as regard as type of PPD diagnosis and degree of cognitive and behavioural symptoms.

The qualitative visual assessment of PET images by a nuclear medicine specialist held an accuracy of 0.84 (95% CI: 0.72, 0.93) with

sensitivity of 0.89 and specificity of 0.75.

3.2. Data driven semiquantitative analysis of [18]FDG-PET images

The 3D surface projections of the SUVr mean values (corrected for PVE) of the bvFTD and PPD groups reported in Fig. 1 depict general views of the hypometabolic areas per disease group. They show that hypometabolism is present in similar areas of the brain in the two groups, mainly the temporal and parietal regions, while a diffuse and severe hypometabolism of the frontal lobe was evident in the bvFTD group.

Whole group PCA of the FDG-PET SUVr values revealed a first component explaining 44.8% of the variance, comprising a cluster of regions distributed over the dorsolateral and ventrolateral frontal cortex, the orbitofrontal cortex and the caudate (in the horizontal axis in Fig. 2). The regions contributing to this component are shown in detail in Fig. 1 of the Supplemental Material.

The majority of bvFTD patients clustered on the right side of the axis (red circles in Fig. 2), revealing lower glucose metabolism in regions of the frontal lobe. However, 12/37 (32.4%) of bvFTD patients mapped in the left half of the horizontal axis, indicating a relatively higher brain metabolism in the frontal lobe regions compared with the right half axis. Analysis of the clinical characteristics of these patients showed that 4 had signs of motoneuron disease (3 sporadic, and 1 c9orf72 +), 2 had gene mutations without motoneuron disease (1 c9orf72, 1 GRN), and 3 had isolated temporal lobe hypometabolism with relative sparing of the frontal cortex. There were no differences in the demographic or other clinical variables between this subgroup and the other bvFTD patients. The three remaining patients of the six genetic cases of bvFTD clustered in the vertical axis (1 c9orf72) and on the right side (1 GRN and 1 c9orf72).

Patients in the PPD group clustered mainly in the left half of the axis (black triangles) identifying patients with relatively higher glucose metabolism in frontal and caudate regions. There were a few patients in the PPD group ($n = 5$) with lower FDG-SUVr values in the frontal regions. These 5 patients (age at onset: 59.8 ± 13.7 years; disease duration: 4 ± 2 years) received a diagnosis of late-onset BD ($n = 2$), UDD ($n = 2$), or GAD ($n = 1$). There were no differences in the demographic, clinical or behavioral characteristics between these and the other 15 PPD patients.

The second PCA component is expressed in the vertical axis of Fig. 2 and corresponds to the regional SUVr values of the bilateral cuneus, which explained 17% of the variance. Interestingly, in this component all but four of the PPD patients clustered in the upper half of the axis, having lower FDG SUVr values; the bvFTD patients, on the other hand, did not segregate along this axis, showing instead higher (lower side) and lower (upper side) glucose metabolism in the primary visual cortex.

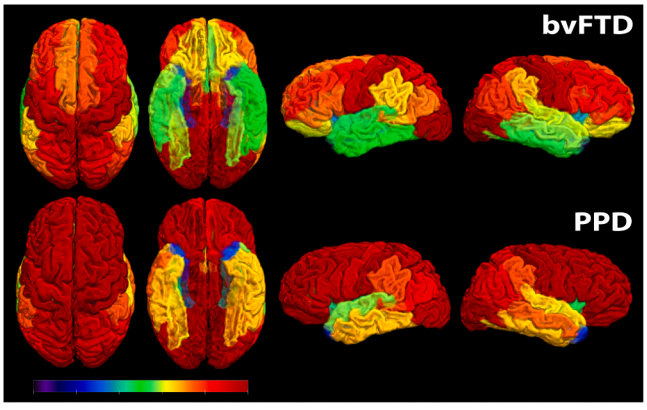

Fig. 1. 3D surface projection of mean regional SUVr values (corrected for PVE) showing (l to r) superior, inferior, right and left projections in bvFTD (top row) and PPD (bottom row). Black-blu-dark green: low FDG uptake (definite hypometabolism); light green-yellow: intermediate FDG uptake (low-grade hypometabolism); red-orange: high FDG uptake (preserved metabolism).

We also divided patients into three groups (left, middle, and right columns in Fig. 2) according to the coordinates of the first principal component as a visual exemplification of the regional patterns of PCA-based hypometabolism.

The regions identified by the first PCA component (dorsolateral, ventrolateral, orbitofrontal regions and caudate) were used to create a linear regression model for subjects classification. The ROC curve is shown in Fig. 3. The model classifies bvFTD versus PPD patients with an accuracy of 0.91 (95% CI: 0.81, 0.97), a sensitivity of 0.95 and specificity of 0.85.

The metabolism values of dorsolateral, ventrolateral, orbitofrontal regions and caudate were also used, one by one, in a linear regression model where the dependent variables were the cognitive/neuropsychiatric features. After Bonferroni correction for multiple testing, the model with the bilateral superior frontal and caudal middle frontal regions showed a significant association with apathy ($p = 0.002$).

4. Discussion

Despite their cognitive and behavioral similarities, brain glucose hypometabolism of the dorsolateral and ventrolateral frontal cortex, the orbito-frontal cortex and the caudate explained almost 45% of the variance among patients with possible bvFTD and could distinguished with very good accuracy patients with probable/definite bvFTD or late onset primary psychiatric disorders. This spatial pattern of glucose hypometabolism along with relatively preserved or increased metabolism in the primary occipital cortex is the metabolic signature of frontotemporal neurodegeneration. Selected cases with genetic bvFTD and/or motoneuron signs showed hypometabolism of the parietal regions. On a qualitative level, almost 50% of patients with late-onset psychiatric disorders mimicking bvFTD had mild hypometabolism in the parietal and/or anterior cingulate cortex, a finding that could represent a diagnostic challenge in a few patients, particularly genetic cases of bvFTD with psychiatric presentation.

4.1. Metabolic patterns in bvFTD

FDG-PET has been reported to have high accuracy in differentiating bvFTD from other neurodegenerative diseases (Dukart et al., 2011; Kerklaan et al., 2014; Vijverberg et al., 2016), but it is not always resolutive when differentiating it from acquired behavioral disease. It is recommended in uncertain/atypical presentation of early-onset dementia as it can improve diagnosis compared with structural MRI, in particular for monitoring neurodegenerative progression over time (Ducharme et al., 2020). While a completely spared FDG-PET suggests an alternative diagnosis to bvFTD, an atypical scan should not be overinterpreted given that FDG-PET specificity has been reported to range from 68 to 97%, and sensitivity from 40 to 90% in bvFTD (Foster et al., 2007; Gossye et al., 2019; Kerklaan et al., 2014; Vijverberg et al., 2016). Different patterns of glucose hypometabolism in bvFTD have been reported: predominant frontal abnormalities (Foster et al., 2007; Kipps et al., 2009), pure temporal involvement (Cerami et al., 2016), parietal hypometabolism, and an almost normal scan (Kerklaan et al., 2014; Kipps et al., 2009; Solje et al., 2015). This heterogeneity reflects different spatial distributions of neurodegeneration and/or different pathological brain changes. The results of our study suggest that at least some of the atypical patterns of hypometabolism are associated with bvFTD-related gene mutations or bvFTD plus motor neuron disease.

Those bvFTD patients who are carriers of gene mutations, particularly c9orf72 expansion, have atypical progression and presentation. Sometimes they may be slowly progressive and have a normal structural and/or metabolic imaging scan, and therefore a phenocopy syndrome of bvFTD (Khan et al., 2012). Solje et al. reported normal/atypical brain PET/SPECT scan in 17.6% (3/17) of c9orf72-bvFTD patients (two

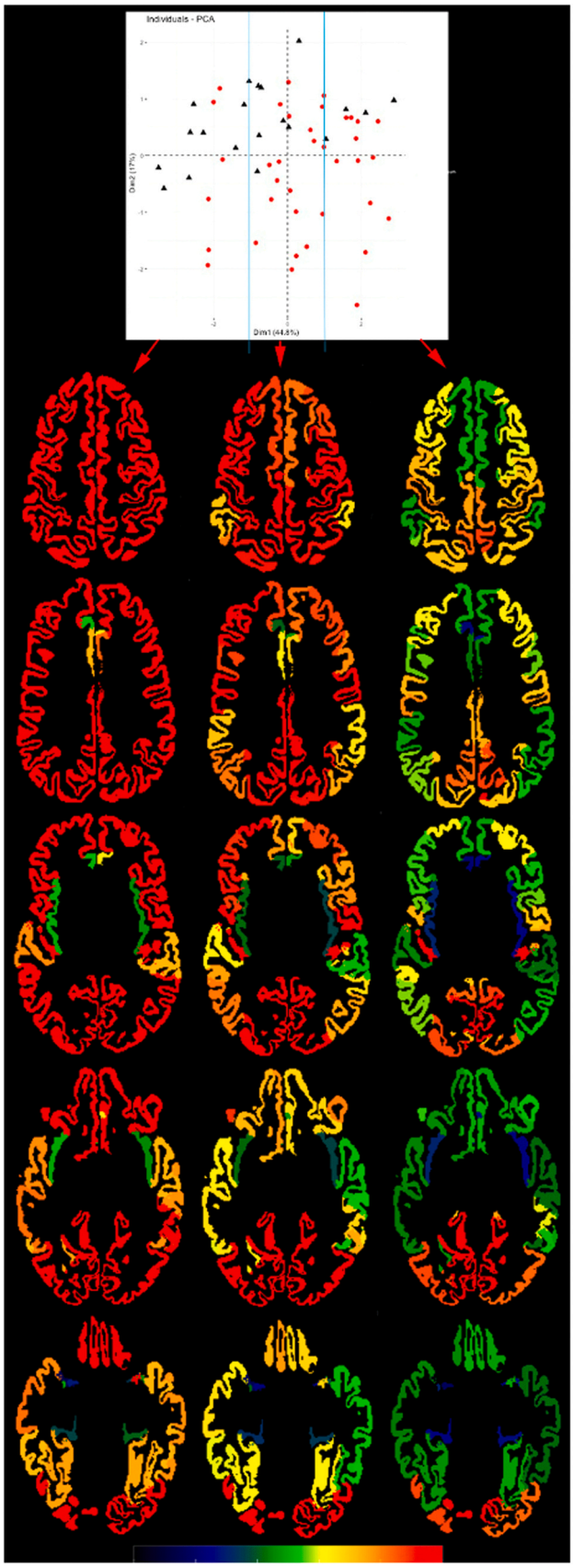

(caption on next column)

Fig. 2. Image (a) depicts the results of the PCA of the FDG-PET SUVr values showing a first component (Dim1) explaining 44.8% of the variance (black triangles = PPD patients, red dots = bvFTD patients) and corresponding to a cluster of frontal regions and caudate nuclei. Image (b) shows the mean SUVr values (PVE corrected) of patients (BvFTD+PPD) divided into three groups (left, middle and right columns) according to the coordinates of the first principal component. Black-blu-dark green: low FDG uptake (definite hypometabolism); light green-yellow: intermediate FDG uptake (low-grade hypometabolism); red-orange: high FDG uptake (preserved metabolism).

normal scans and one bilateral parietal hypoperfusion) (Solje et al., 2015). In their pilot study, Devenney et al. described low FDG uptake in the parietal lobe of one c9orf72 bvFTD case, while another presented a diffuse cortical hypometabolism (including the parietal regions, thalamus, and cerebellum), and half of the patients (n = 3/6) showed frontal and/or temporal hypometabolism (Devenney et al., 2014).

In contrast, hypermetabolism in the occipital cortex, pre- and postcentral gyri and subcortical structures associated with brain hypometabolism in the frontal regions has been described in two c9orf72 bvFTD patients compared with controls in a small FDG-PET study assessing metabolic patterns at the individual level (Castelnovo et al., 2019).

Our results confirm previous heterogeneous findings in genetic bvFTD cases by detecting atypical hypometabolism in 3/6 patients with involvement of the parietal cortex (1 c9orf72 and 1 GRN) or with a normal scan (1 c9orf72).

To the best of our knowledge, there are at present no studies assessing differences in regional brain metabolism across groups of patients with different bvFTD-related gene mutations. However, a few MRI studies found that some bvFTD-related gene mutations have typical patterns of regional brain atrophy: GRN is associated with asymmetric temporo-parietal atrophy, and c9orf72 expansion with diffuse grey matter atrophy, while TAU is typically associated with mesial temporal atrophy.(Fumagalli et al., 2018) However, also in MRI studies, heterogeneous findings have been described in c9orf72 carriers compared with sporadic bvFTD (Cash et al., 2018; Lee et al., 2017; Whitwell et al., 2012) and controls,(Mahoney et al., 2012) including widespread reduction in cortical thickness (Cash et al., 2018; Floeter et al., 2016; Mahoney et al., 2012; Whitwell et al., 2012), worse atrophy in the anterior cingulate (Devenney et al., 2014) and parietal cortex (Cash et al., 2018; Whitwell et al., 2012)' and in the thalamus and superior cerebellar cortex (Cash et al., 2018).

Few studies have compared neuroimaging findings from bvFTD patients with and without motoneuron signs. Typical FDG-PET imaging of MND shows hypometabolic alterations to the frontal lobe associated with significant hypermetabolism of the posterior occipital and middle temporal cortex, cerebellum, midbrain and cortico-striatal tracts in patients with cognitive decline compared with controls (Canosa et al., 2016; Kassubek and Pagani, 2019).

Consistent with the literature, the results of our study confirm that a few patients with probable/definite bvFTD may present atypical spatial patterns of brain metabolism, being less pronounced in the dorsolateral frontal cortex, but more pronounced in the posterior regions, and that these patients may have genetic mutations (c9orf72 and GRN) or sporadic forms of bvFTD-MND. This possibility should be kept in mind when applying current diagnostic criteria for probable bvFTD, which include the presence of frontotemporal neuroimaging abnormalities. Moreover, genetic bvFTD cases may be easily misdiagnosed due to unusual clinical presentation with behavioral disturbances not recognized in the current diagnostic criteria, such as psychosis. The combination of atypical clinical presentation and atypical neuroimaging findings increases the risk of misdiagnosis.

As far as the finding of occipital hypermetabolism found in some patients with bvFTD (Castelnovo et al., 2019), and confirmed with the our results of PCA analysis, we suggest that higher occipital metabolism in bvFTD may be due to disinhibited behaviour and lack of maintenance

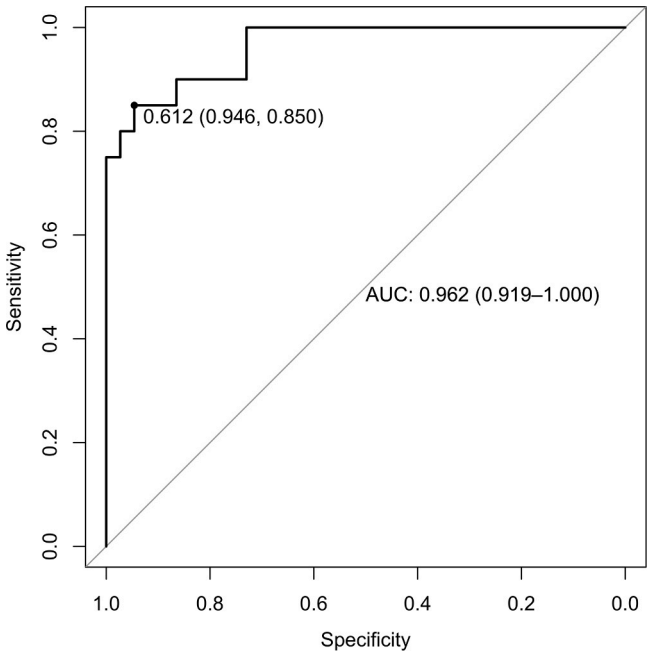

Fig. 3. ROC curve obtained with a regression model for subjects classification created using the SUVr values of the regions identified by the PCA first component (dorsolateral, ventrolateral, orbitofrontal regions and caudate).

of close eyes during the scan in bvFTD patients.

4.2. FDG-PET in primary psychiatric disorders with late-onset frontal lobe syndrome

Some patients with late-onset behavioral and/or cognitive frontal lobe syndrome meeting the diagnostic criteria for possible bvFTD may lack significant frontotemporal atrophy or hypometabolism, and may not get worse on functional and cognitive assessments over time. This condition is also known in the literature as bvFTD phenocopy syndrome (Devenney et al., 2018; Gossink et al., 2016; Kipps et al., 2009, 2007; Vijverberg et al., 2017). The etiology is heterogeneous and includes late-onset psychiatric disorders, worsening of a pre-existing subtle psychiatric disorder, and benign forms of bvFTD, also with genetic mutations (Khan et al., 2012; Kipps et al., 2010; Vijverberg et al., 2017). For the purposes of this study we included a selective subgroup of bvFTD mimickers for whom a differential diagnosis is particularly challenging, such as those with possible bvFTD based on clinical manifestations of a frontal lobe syndrome, recent diagnosis of a late-onset primary psychiatric disorder, and absent or minimal frontal lobe atrophy or hypometabolism, according to previous studies by Vijverberg and collaborators (Vijverberg et al., 2016; Vijverberg et al., 2017). The accuracy of neuroimaging in discriminating between bvFTD and clinical "phenocopies" is currently under study. FDG-PET was shown to have high specificity (92%) in a group of 52 patients with clinical suspected bvFTD (Neary et al., 1998), but normal structural (MRI) imaging. Kerklaan et al. reported that brain metabolism could discriminate bvFTD from mimickers, such as psychiatric disorders and phenocopy syndrome (Kerklaan et al., 2014).

In contrast, Vijverberg et al. found relatively low specificity (68%) when evaluating the ability of FDG-PET to differentiate bvFTD from non-bvFTD (late-onset frontal lobe syndrome) based on follow-up diagnosis. The lack of specificity was due to false-positive scans among non-bvFTD patients (psychiatric disorders and a variety of neurological diseases): 40% of these conditions were primary psychiatric disorders and presented mainly with bilateral frontal and temporal lobe hypometabolism, with a few also showing decreased metabolism in the parietal regions (right<left side) (Vijverberg et al., 2016). In line with their study, our results revealed the presence of abnormalities in brain glucose metabolism in almost 50% of possible bvFTD cases with a psychiatric diagnosis, and in our group of PPD patients hypometabolism was distributed over the anterior cingulate and superior parietal regions.

Furthermore, MRI visual ratings revealed MTA and GCA to be significantly higher in bvFTD compared with PPD, supporting previous suggestion that selected brain atrophy in temporal regions assessed with a visual rating scale may be a good indicator of neurodegenerative disorder in a late-onset behavioral change cohort (Vijverberg et al., 2016). On the other hand, an ASL-MRI study (Steketee et al., 2016) found right temporal lobe atrophy in both bvFTD phenocopy syndrome (with apparently spared neuroimaging and no decline over 1 year) and bvFTD. There was also less atrophy in the right hippocampal formation and the amygdala in bvFTD phenocopy syndrome than in bvFTD (Steketee et al., 2016).

Koedam scores turned out to be unable to distinguish the two group, which might be due to the co-presence of structural and metabolic parietal alteration in both groups, which was more extended in genetic bvFTD and bvFTD plus MND, as the PCA results showed.

It is worth noting that we also found the caudate to play a role in differential diagnosis in that it is more compromised in bvFTD, which is supported by the findings of a PET-MRI study showing that the caudate is hypometabolic in bvFTD compared with late-onset BD (Delvecchio et al., 2019). In fact, there are few neuroimaging studies comparing psychiatric disease with bvFTD, and they confirm the presence of minimal alterations in psychiatric disease, mainly atrophy of the ventrolateral prefrontal cortex, while dorsolateral prefrontal cortex and temporal cortex atrophy and hypometabolism was found in bvFTD (Baez et al., 2019; Delvecchio et al., 2019; Nascimento et al., 2019).

5. Conclusions

A major limitation of the study is the lack of a healthy control group for semiquantative data analysis of brain metabolism. Although visual analysis of brain PET scan was performed by comparing each individual scan with a dataset of age-matched normal controls applying regional z-scores, semiquantitative analysis of brain metabolism was available only for patients' groups. This limits the considerations on the degree of regional hypometabolism found in a subset of PPD.

In conclusion, given the diagnostic challenge of differentiating neurodegenerative bvFTD from late-onset frontal lobe syndrome in newly diagnosed psychiatric disorders, we suggest that detection of significant hypometabolism in dorsolateral/orbitofrontal regions and the caudate nucleus may increase accuracy. In contrast, we do not consider a mild degree of metabolic alteration in the anterior cingulate cortex and a wider range of hypometabolism in the superior parietal and superior-temporal regions to be useful in differential diagnosis since these may be detected in some genetic forms of bvFTD and in late-onset frontal lobe syndrome due to psychiatric diseases.

Funding

The PET/MRI acquisition system of the University Hospital of Padua was funded by the "Fondazione Cassa di Risparmio di Padova e Rovigo" and co-funded by the University Hospital of Padua. CB received a grant by the Associazione Italiana Ricerca Alzheimer Onlus (AIRAlzh) funded by Consorzio Nazionale delle Cooperative di Consumatori (COOP ITALIA S.C.).

CRediT authorship contribution statement

Cagnin Annachiara: Writing – review & editing, Writing – original draft, Supervision, Resources, Data curation, Conceptualization. **Pigato Giorgio:** Supervision, Data curation, Conceptualization. **Campi Cristina:** Supervision, Software, Methodology, Formal analysis. **Cecchin Diego:** Writing – review & editing, Supervision, Methodology,

Investigation, Formal analysis, Data curation, Conceptualization. **mozzetta stefano:** Investigation, Formal analysis, Data curation. **gabelli carlo:** Data curation. **Anglani Maria Giulia:** Investigation, Formal analysis, Data curation. **Bussè Cinzia:** Resources, Data curation. **Zorzi Giovanni:** Methodology, Formal analysis, Data curation. **Roiter Beatrice:** Data curation. **Pettenuzzo Ilaria:** Formal analysis, Data curation.

Declaration of Competing Interest

No conflict of interest to be declared.

Appendix A. Supporting information

Supplementary data associated with this article can be found in the online version at doi:10.1016/j.neurobiolaging.2024.01.015.

References

Baez, S., Pinasco, C., Roca, M., Ferrari, J., Couto, B., García-Cordero, I., Ibañez, A., Cruz, F., Reyes, P., Matallana, D., Manes, F., Cetcovich, M., Torralva, T., 2019. Brain structural correlates of executive and social cognition profiles in behavioral variant frontotemporal dementia and elderly bipolar disorder. Neuropsychologia 126, 159–169. https://doi.org/10.1016/j.neuropsychologia.2017.02.012.

Caffarra, P., Vezzadini, G., Dieci, F., Zonato, F., Venneri, A., 2002. Rey-Osterrieth complex figure: normative values in an Italian population sample. Neurol. Sci. Off. J. Ital. Neurol. Soc. Ital. Soc. Clin. Neurophysiol. 22, 443–447. https://doi.org/10.1007/s100720200003.

Cagnin, A., Formentin, C., Pompanin, S., Zarantonello, G., Jelcic, N., Venneri, A., Ermani, M., 2014. Simple motor stereotypies are not specific features of behavioural frontotemporal dementia. J. Neurol. Neurosurg. Psychiatry 85, 943–944. https://doi.org/10.1136/jnnp-2013-307471.

Canosa, A., Pagani, M., Cistaro, A., Montuschi, A., Iazzolino, B., Fania, P., Cammarosano, S., Ilardi, A., Moglia, C., Calvo, A., Chiò, A., 2016. F-FDG-PET correlates of cognitive impairment in ALS. Neurology 86. https://doi.org/10.1212/WNL.0000000000002242.

Carlesimo, G.A., Caltagirone, C., Gainotti, G., 1996. The mental deterioration battery: normative data, diagnostic reliability and qualitative analyses of cognitive impairment. The group for the standardization of the mental deterioration battery. Eur. Neurol. 36, 378–384. https://doi.org/10.1159/000117297.

Cash, D.M., Bocchetta, M., Thomas, D.L., Dick, K.M., van Swieten, J.C., Borroni, B., Galimberti, D., Masellis, M., Tartaglia, M.C., Rowe, J.B., Graff, C., Tagliavini, F., Frisoni, G.B., Laforce, R., Finger, E., de Mendonça, A., Sorbi, S., Rossor, M.N., Ourselin, S., Rohrer, J.D., 2018. Patterns of gray matter atrophy in genetic frontotemporal dementia: results from the GENFI study. Neurobiol. Aging 62, 191–196. https://doi.org/10.1016/j.neurobiolaging.2017.10.008.

Castelnovo, V., Caminiti, S.P., Riva, N., Magnani, G., Silani, V., Perani, D., 2019. Heterogeneous brain FDG-PET metabolic patterns in patients with C9orf72 mutation. Neurol. Sci. 40, 515–521. https://doi.org/10.1007/s10072-018-3685-7.

Cecchin, D., Barthel, H., Poggiali, D., Cagnin, A., Tiepolt, S., Zucchetta, P., Turco, P., Gallo, P., Frigo, A.C., Sabri, O., Bui, F., 2017. A new integrated dual time-point amyloid PET/MRI data analysis method. Eur. J. Nucl. Med. Mol. Imaging 44, 2060–2072. https://doi.org/10.1007/s00259-017-3750-0.

Cerami, C., Dodich, A., Lettieri, G., Iannaccone, S., Magnani, G., Marcone, A., Gianolli, L., Cappa, S.F., Perani, D., 2016. Different FDG-PET metabolic patterns at single-subject level in the behavioral variant of fronto-temporal dementia. Cortex 83, 101–112. https://doi.org/10.1016/j.cortex.2016.07.008.

Cummings, J.L., Mega, M., Gray, K., Rosenberg-Thompson, S., Carusi, D.A., Gornbein, J., 1994. The neuropsychiatric inventory: comprehensive assessment of psychopathology in dementia. Neurology 44, 2308–2314. https://doi.org/10.1212/wnl.44.12.2308.

Delvecchio, G., Mandolini, G.M., Arighi, A., Prunas, C., Mauri, C.M., Pietroboni, A.M., Marotta, G., Cinnante, C.M., Triulzi, F.M., Galimberti, D., Scarpini, E., Altamura, A. C., Brambilla, P., 2019. Structural and metabolic cerebral alterations between elderly bipolar disorder and behavioural variant frontotemporal dementia: a combined MRI-PET study. Aust. N. Z. J. Psychiatry 53, 413–423. https://doi.org/10.1177/0004867418815976.

Devenney, E., Hornberger, M., Irish, M., Mioshi, E., Burrell, J., Tan, R., Kiernan, M.C., Hodges, J.R., 2014. Frontotemporal dementia associated with the C9ORF72 mutation: a unique clinical profile. JAMA Neurol. 71, 331–339. https://doi.org/10.1001/jamaneurol.2013.6002.

Devenney, E., Swinn, T., Mioshi, E., Hornberger, M., Dawson, K.E., Mead, S., Rowe, J.B., Hodges, J.R., 2018. The behavioural variant frontotemporal dementia phenocopy syndrome is a distinct entity - evidence from a longitudinal study. BMC Neurol. https://doi.org/10.1186/s12883-018-1060-1.

Dubois, B., Slachevsky, A., Litvan, I., Pillon, B., 2000. The FAB: a frontal assessment battery at bedside. Neurology 55, 1621–1626. https://doi.org/10.1212/WNL.55.11.1621.

Ducharme, Dols, S., Laforce, A., Devenney, R., Kumfor, E., Seelaar, F., Gossink, H., Stock, F., Van Den, J., Trieu, Dallaire-the, C., Onyike, C., Caramelli, C., Souza, P., De, L.C., Landin-romero, R., Piguet, O., Santillo, A., Waldo, M.L., Ellayosyula, R., Pasquier, F., Galimberti, D., Scarpini, E., 2020. OUP accepted manuscript. Brain. https://doi.org/10.1093/brain/awaa018.

Dukart, J., Mueller, K., Horstmann, A., Barthel, H., Möller, H.E., Villringer, A., Sabri, O., Schroeter, M.L., 2011. Combined evaluation of FDG-PET and MRI improves detection and differentiation of dementia. PLoS One 6, e18111.

Fazekas, F., Chawluk, J.B., Alavi, A., Hurtig, H.I., Zimmerman, R.A., 1987. MR signal abnormalities at 1.5 T in Alzheimer's dementia and normal aging. Am. J. Roentgenol. 149, 351–356. https://doi.org/10.2214/ajr.149.2.351.

Floeter, M.K., Bageac, D., Danielian, L.E., Braun, L.E., Traynor, B.J., Kwan, J.Y., 2016. Longitudinal imaging in C9orf72 mutation carriers: relationship to phenotype. NeuroImage Clin. 12, 1035–1043. https://doi.org/10.1016/j.nicl.2016.10.014.

Foster, N.L., Heidebrink, J.L., Clark, C.M., Jagust, W.J., Arnold, S.E., Barbas, N.R., DeCarli, C.S., Scott Turner, R., Koeppe, R.A., Higdon, R., Minoshima, S., 2007. FDG-PET improves accuracy in distinguishing frontotemporal dementia and Alzheimer's disease. Brain 130, 2616–2635. https://doi.org/10.1093/brain/awm177.

Fumagalli, G.G., Basilico, P., Arighi, A., Bocchetta, M., Dick, K.M., Cash, D.M., Harding, S., Mercurio, M., Fenoglio, C., Pietroboni, A.M., Ghezzi, L., Van Swieten, J., Borroni, B., De Mendonça, A., Masellis, M., Tartaglia, M.C., Rowe, J.B., Graff, C., Tagliavini, F., Frisoni, G.B., Laforce, R., Finger, E., Sorbi, S., Scarpini, E., Rohrer, J. D., Galimberti, D., 2018. Distinct patterns of brain atrophy in Genetic Frontotemporal Dementia Initiative (GENFI) cohort revealed by visual rating scales. Alzheimer's Res. Ther. 10 (1–9) https://doi.org/10.1186/s13195-018-0376-9.

Goetz, C.G., Fahn, S., Martinez-Martin, P., Poewe, W., Sampaio, C., Stebbins, G.T., Stern, M.B., Tilley, B.C., Dodel, R., Dubois, B., Holloway, R., Jankovic, J., Kulisevsky, J., Lang, A.E., Lees, A., Leurgans, S., LeWitt, P.A., Nyenhuis, D., Olanow, C.W., Rascol, O., Schrag, A., Teresi, J.A., Van Hilten, J.J., LaPelle, N., 2007. Movement disorder society-sponsored revision of the unified Parkinson's disease rating scale (MDS-UPDRS): process, format, and clinimetric testing plan. Mov. Disord. 22, 41–47. https://doi.org/10.1002/mds.21198.

Gossink, F.T., Dols, A., Kerssens, C.J., Krudop, W.A., Kerklaan, B.J., Scheltens, P., Stek, M.L., Pijnenburg, Y.A.L., 2016. Psychiatric diagnoses underlying the phenocopy syndrome of behavioural variant frontotemporal dementia. J. Neurol., Neurosurg. Psychiatry 87, 64–68. https://doi.org/10.1136/jnnp-2014-308284.

Gossye, H., Van Broeckhoven, C., Engelborghs, S., 2019. The use of biomarkers and genetic screening to diagnose frontotemporal dementia: evidence and clinical implications. Front. Genet. 10, 1–18. https://doi.org/10.3389/fnins.2019.00757.

Hotelling, H., 1933. Analysis of a complex of statistical variables into principal components. J. Educ. Psychol. 24, 417–441. https://doi.org/10.1037/h0071325.

Kassubek, J., Pagani, M., 2019. Imaging in amyotrophic lateral sclerosis: MRI and PET. Curr. Opin. Neurol. 32, 740–746. https://doi.org/10.1097/WCO.0000000000000728.

Katz, S., Ford, A.B., Moskowitz, R.W., Jackson, B.A., Jaffe, M.W., 1963. Studies of Illness in the Aged: the Index of ADL: a standardized measure of biological and psychosocial function. JAMA 185, 914–919. https://doi.org/10.1001/jama.1963.03060120024016.

Kerklaan, B.J., van Berckel, B.N.M., Herholz, K., Dols, A., van der Flier, W.M., Scheltens, P., Pijnenburg, Y.A.L., 2014. The added value of 18-fluorodeoxyglucose-positron emission tomography in the diagnosis of the behavioral variant of frontotemporal dementia. Am. J. Alzheimer's Dis. Other Dement. 29, 607–613. https://doi.org/10.1177/1533317514524811.

Khan, B.K., Yokoyama, J.S., Takada, L.T., Sha, S.J., Rutherford, N.J., Fong, J.C., Karydas, A.M., Wu, T., Ketelle, R.S., Baker, M.C., Hernandez, M.D., Coppola, G., Geschwind, D.H., Rademakers, R., Lee, S.E., Rosen, H.J., Rabinovici, G.D., Seeley, W. W., Rankin, K.P., Boxer, A.L., Miller, B.L., 2012. Atypical, slowly progressive behavioural variant frontotemporal dementia associated with C9ORF72 hexanucleotide expansion. J. Neurol., Neurosurg. Psychiatry 83, 358–364. https://doi.org/10.1136/jnnp-2011-301883.

Kipps, C.M., Davies, R.R., Mitchell, J., Kril, J.J., Halliday, G.M., Hodges, J.R., 2007. Clinical significance of lobar atrophy in frontotemporal dementia: Application of an MRI visual rating scale. Dement. Geriatr. Cogn. Disord. 23, 334–342. https://doi.org/10.1159/000100973.

Kipps, C.M., Hodges, J.R., Fryer, T.D., Nestor, P.J., 2009. Combined magnetic resonance imaging and positron emission tomography brain imaging in behavioural variant frontotemporal degeneration: refining the clinical phenotype. Brain 132, 2566–2578. https://doi.org/10.1093/brain/awp077.

Kipps, C.M., Hodges, J.R., Hornberger, M., 2010. Nonprogressive behavioural frontotemporal dementia: recent developments and clinical implications of the "bvFTD phenocopy syndrome. Curr. Opin. Neurol. 23, 628–632. https://doi.org/10.1097/WCO.0b013e3283404309.

Koedam, E.L.G.E., Lehmann, M., van der Flier, W.M., Scheltens, P., Pijnenburg, Y.A.L., Fox, N., Barkhof, F., Wattjes, M.P., 2011. Visual assessment of posterior atrophy development of a MRI rating scale. Eur. Radiol. 21, 2618–2625. https://doi.org/10.1007/s00330-011-2205-4.

Lawton, M.P., Brody, E.M., 1969. Assessment of older people: self-maintaining and instrumental activities of daily living1. Gerontologist 9, 179–186. https://doi.org/10.1093/geront/9.3_Part_1.179.

Lee, S.E., Sias, A.C., Mandelli, M.L., Brown, J.A., Brown, A.B., Khazenzon, A.M., Vidovszky, A.A., Zanto, T.P., Karydas, A.M., Pribadi, M., Dokuru, D., Coppola, G., Geschwind, D.H., Rademakers, R., Gorno-Tempini, M.L., Rosen, H.J., Miller, B.L., Seeley, W.W., 2017. Network degeneration and dysfunction in presymptomatic C9ORF72 expansion carriers. NeuroImage: Clin. 14, 286–297. https://doi.org/10.1016/j.nicl.2016.12.006.

Mahoney, C.J., Beck, J., Rohrer, J.D., Lashley, T., Mok, K., Shakespeare, T., Yeatman, T., Warrington, E.K., Schott, J.M., Fox, N.C., Rossor, M.N., Hardy, J., Collinge, J., Revesz, T., Mead, S., Warren, J.D., 2012. Frontotemporal dementia with the

C9ORF72 hexanucleotide repeat expansion: clinical, neuroanatomical and neuropathological features. Brain 135, 736–750. https://doi.org/10.1093/brain/awr361.

Minoshima, S., Frey, K.A., Koeppe, R.A., Foster, N.L., Kuhl, D.E., 1995. A diagnostic approach in Alzheimer's disease using three-dimensional stereotactic surface projections of fluorine-18-FDG PET. J. Nucl. Med. Off. Pibl. Soc. Nucl. Med. 36, 1238–1248.

Nascimento, C., Villela Nunes, P., Diehl Rodriguez, R., Takada, L., Kimie Suemoto, C., Tenenholz Grinberg, L., Nitrini, R., Lafer, B., 2019. A review on shared clinical and molecular mechanisms between bipolar disorder and frontotemporal dementia. Prog. Neuro-Psychopharmacol. Biol. Psychiatry 93, 269–283. https://doi.org/10.1016/j.pnpbp.2019.04.008.

Neary, D., Snowden, J.S., Gustafson, L., Passant, U., Stuss, D., Black, S., Freedman, M., Kertesz, A., Robert, P.H., Albert, M., Boone, K., Miller, B.L., Cummings, J., Benson, D.F., 1998. Frontotemporal lobar degeneration: a consensus on clinical diagnostic criteria. Neurology 51, 1546–1554. https://doi.org/10.1212/wnl.51.6.1546.

Pasquier, F., Leys, D., Weerts, J.G.E., Mounier-Vehier, F., Barkhof, F., Scheltens, P., 1996. Inter-and intraobserver reproducibility of cerebral atrophy assessment on MRI scans with hemispheric infarcts. Eur. Neurol. 36, 268–272. https://doi.org/10.1159/000117270.

Rascovsky, K., Hodges, J.R., Knopman, D., Mendez, M.F., Kramer, J.H., Neuhaus, J., Van Swieten, J.C., Seelaar, H., Dopper, E.G.P., Onyike, C.U., Hillis, A.E., Josephs, K.A., Boeve, B.F., Kertesz, A., Seeley, W.W., Rankin, K.P., Johnson, J.K., Gorno-Tempini, M.L., Rosen, H., Prioleau-Latham, C.E., Lee, A., Kipps, C.M., Lillo, P., Piguet, O., Rohrer, J.D., Rossor, M.N., Warren, J.D., Fox, N.C., Galasko, D., Salmon, D.P., Black, S.E., Mesulam, M., Weintraub, S., Dickerson, B.C., Diehl-Schmid, J., Pasquier, F., Deramecourt, V., Lebert, F., Pijnenburg, Y., Chow, T.W., Manes, F., Grafman, J., Cappa, S.F., Freedman, M., Grossman, M., Miller, B.L., 2011. Sensitivity of revised diagnostic criteria for the behavioural variant of frontotemporal dementia. Brain 134, 2456–2477. https://doi.org/10.1093/brain/awr179.

Sala, Della, Laiacona, S., Spinnler, M., Ubezio, C, H., 1992. A cancellation test: its reliability in assessing attentional deficits in Alzheimer's disease. Psychol. Med. 22, 885–901. https://doi.org/10.1017/s0033291700038460.

Scheltens, P., Leys, D., Barkhof, F., Huglo, D., Weinstein, H.C., Vermersch, P., Kuiper, M., Steinling, M., Wolters, E.C., Valk, J., 1992. Atrophy of medial temporal lobes on MRI in "probable" Alzheimer's disease and normal ageing: diagnostic value and neuropsychological correlates. J. Neurol., Neurosurg., Psychiatry 55, 967–972. https://doi.org/10.1136/jnnp.55.10.967.

Scheltens, P., Launer, L.J., Barkhof, F., Weinstein, H.C., van Gool, W.A., 1995. Visual assessment of medial temporal lobe atrophy on magnetic resonance imaging: interobserver reliability. J. Neurol. 242, 557–560. https://doi.org/10.1007/BF00868807.

Sheehan, D.V., Lecrubier, Y., Sheehan, K.H., Amorim, P., Janavs, J., Weiller, E., Hergueta, T., Baker, R., Dunbar, G.C., 1998. The Mini-International Neuropsychiatric Interview (M.I.N.I.): the development and validation of a structured diagnostic psychiatric interview for DSM-IV and ICD-10. J. Clin. Psychiatry 59 Suppl 2, 22–57.

Solje, E., Aaltokallio, H., Koivumaa-Honkanen, H., Suhonen, N.M., Moilanen, V., Kiviharju, A., Traynor, B., Tienari, P.J., Hartikainen, P., Remes, A.M., 2015. The phenotype of the C9ORF72 expansion carriers according to revised criteria for bvFTD. PLoS ONE 10, 1–9. https://doi.org/10.1371/journal.pone.0131817.

Steketee, R.M.E., Meijboom, R., Bron, E.E., Osse, R.J., De Koning, I., Jiskoot, L.C., Klein, S., De Jong, F.J., Van Der Lugt, A., Van Swieten, J.C., Smits, M., 2016. Structural and functional brain abnormalities place phenocopy frontotemporal dementia (FTD) in the FTD spectrum. NeuroImage: Clin. 11, 595–605. https://doi.org/10.1016/j.nicl.2016.03.019.

Varrone, A., Asenbaum, S., Vander Borght, T., Booij, J., Nobili, F., Någren, K., Darcourt, J., Kapucu, O.L., Tatsch, K., Bartenstein, P., Van Laere, K., 2009. EANM procedure guidelines for PET brain imaging using [18F]FDG, version 2. Eur. J. Nucl. Med. Mol. Imaging 36, 2103–2110. https://doi.org/10.1007/s00259-009-1264-0.

Vijverberg, E.G.B., Wattjes, M.P., Dols, A., Krudop, W.A., Möller, C., Peters, A., Kerssens, C.J., Gossink, F., Prins, N.D., Stek, M.L., Scheltens, P., van Berckel, B.N.M., Barkhof, F., Pijnenburg, Y.A.L., 2016. Diagnostic Accuracy of MRI and Additional [18F]FDG-PET for Behavioral Variant Frontotemporal Dementia in Patients with Late Onset Behavioral Changes. J. Alzheimer's Dis. 53, 1287–1297. https://doi.org/10.3233/JAD-160285.

Vijverberg, E.G.B., Gossink, F., Krudop, W., Sikkes, S., Kerssens, C., Prins, N., Stek, M., Scheltens, P., Pijnenburg, Y., Dols, A., 2017. The diagnostic challenge of y the y Late-onset frontal lobe syndrome: Clinical predictors for primary psychiatric disorders versus behavioral variant frontotemporal dementia. J. Clin. Psychiatry 78, e1197–e1203. https://doi.org/10.4088/JCP.16m11078.

Whitwell, J.L., Weigand, S.D., Boeve, B.F., Senjem, M.L., Gunter, J.L., Dejesus-Hernandez, M., Rutherford, N.J., Baker, M., Knopman, D.S., Wszolek, Z.K., Parisi, J. E., Dickson, D.W., Petersen, R.C., Rademakers, R., Jack, C.R., Josephs, K.A., 2012. Neuroimaging signatures of frontotemporal dementia genetics: C9ORF72, tau, progranulin and sporadics. Brain 135, 794–806. https://doi.org/10.1093/brain/aws001.